Journal of Hazardous Materials 166 (2009) 619–627

Contents lists available at ScienceDirect

Journal of Hazardous Materials

journal homepage: www.elsevier.com/locate/jhazmat

Continuous elimination of Pb^{2+}, Cu^{2+}, Zn^{2+}, H^+ and NH_4^+ from acidic waters by ionic exchange on natural zeolites

Benjamin Calvo[a], Laureano Canoira[a,*], Fernando Morante[b], José M. Martínez-Bedia[a], Carlos Vinagre[a], Jerónimo-Emilio García-González[a], Jan Elsen[c], Ramon Alcantara[a]

[a] E.T.S. Ingenieros de Minas, Universidad Politécnica de Madrid, Rios Rosas 21, 28003 Madrid, Spain
[b] Instituto de Ciencias Químicas y Ambientales, Escuela Superior Politécnica del Litoral, P.O. Box 09-01-5863, Guayaquil, Ecuador
[c] Physico-Chemische Geologie, Katholieke Universiteit Leuven, Celestijnenlaan 200E, B-3001, Heverlee, Belgium

ARTICLE INFO

Article history:
Received 27 May 2008
Received in revised form 21 October 2008
Accepted 22 November 2008
Available online 3 December 2008

Keywords:
Natural zeolites
Breakthrough curves
Acid mine drainage
Wastewater

ABSTRACT

A study of breakthrough curves for cations usually found in acid mine drainage (Pb^{2+}, Cu^{2+}, Zn^{2+} and H^+) and municipal wastewater (NH_4^+) have been conducted on some natural zeolitic tuffs. The zeolitic tuffs used in this study are: three zeolitic tuffs from Cayo Formation, Guayaquil (Ecuador), characterized by X-ray diffraction as clinoptilolite (sample CLI-1) and heulandite (samples HEU-1 and HEU-2)-rich tuffs, and two zeolitic tuffs from Parnaiba Basin, Belem do Pará (Brazil), characterized as stilbite-rich tuffs (samples STI-1 and STI-2). The clinoptilolite sample CLI-1 shows an exceedingly good exchange capacities for Pb^{2+} and NH_4^+ as received, and also a very high exchange capacity for Cu^{2+} and Zn^{2+} when conditioned with 2 M sodium chloride, with much higher values than those reported in the literature for other clinioptilolite ores. A general order of effective cation exchange capacity could be inferred from breakthrough curves on these zeolitic tuffs:

$$CLI-1 > HEU-2 > HEU-1 > STI-2$$

Since it is true for most of the cations studied.

1. Introduction

Zeolites are crystalline aluminosilicates with a three-dimensional framework structure based on repeated units of silicon–oxygen (SiO_4) and aluminum–oxygen (AlO_4) tetrahedra. They contain exchangeable alkaline and alkaline-earth metal cations such as K^+, Na^+, Ca^{2+} and Mg^{2+} that maintain charge neutrality. The microporous crystalline structure of zeolites is able to exchange ionic species that have diameters that fit through the entry ports of internal zeolite framework, while larger species are excluded, giving rise to ion sieving properties that are exploited in a wide range of commercial applications.

Clinoptilolite is the most abundant natural zeolite that occurs in relatively large mineable sedimentary deposits in sufficiently high purity in many parts of the world [1,2]. This zeolite has found applications in the recovery of cesium [3] and thorium [4] from radioactive wastewater, treatment of metal contaminated effluents [5,6], and effective removal of lead, cadmium [7] and ammonium [8] from polluted effluents. It has also been used in China, Greece, Bulgaria and Cuba as a mineral admixture in concrete [9–11]. Stilbite is commonly found as a vein mineral or locally as a replacement product in volcanogenic rock, associated with minerals of the heulandite or laumontite group [12].

The acid mine drainage (AMD) is a problem in some actual mining operations and for some abandoned mines. The acidity of the waters originates from the oxidation of the iron sulfide minerals through a complex combination of chemical and bacterial action, primarily with pyrite to form sulphuric acid. The acidic mine water leaches metal cations from the contacted minerals [13]. In the Iberian pyritic belt of the South of Spain and Portugal, the main cations leached by this process are Pb^{2+}, Cu^{2+} and Zn^{2+}. Treatment process for the removal of these heavy metal cations from AMD include coagulation, carbon adsorption, ion exchange, precipitation and reverse osmosis [14]. The ion exchange processes are probably the most attractive among these methods, since their application is simple, and they require relatively mild operating conditions, although the cost of ion exchange materials and regeneration is the limiting factor [5]. For this reason, it is important to look for low-cost ion exchange materials as natural zeolites that could replace synthetic ion exchange resins. Natural zeolites are the most important

* Corresponding author. Tel.: +34 91 336 6949; fax: +34 91 336 6948.
E-mail addresses: laureano.canoira.lopez@upm.es, laucan@qyc.upm.es (L. Canoira), fmorante@espol.edu.ec (F. Morante), jan.elsen@geo.kuleuven.be (J. Elsen).

0304-3894/$ – see front matter © 2008 Elsevier B.V. All rights reserved.
doi:10.1016/j.jhazmat.2008.11.087

Table 1
Mineralogical composition of the zeolitic tuffs by X-ray diffraction.

Sample	Main phases	Minor phases	Clinoptilolite–heulandite				Stilbite d = 9.12 Å
			d = 8.98 Å		d = 3.97 Å		
			(1)	(2)	(1)	(2)	
HEU-1	Qz, Fd, Cli-Heu	Clay, Cal	91	0	86	21	–
HEU-2	Qz, Fd, Cli-Heu	Clay	104	0	144	27	–
CLI-1	Qz, Cli-Heu, Cal, Fd	Clay	156	158	170	156	–
STI-2	Qz, St	Clay	–	–	–	–	825
STI-1	Qz, St	Clay	–	–	–	–	593
CLI-2[a]	Qz, Cli-Heu, Cal, Fd	Clay	191		181	–	–
CLI-2[b]	Qz, Cli-Heu, Cal, Fd	Clay	171		119	–	–
CLI-1[c]	Qz, Cli-Heu, Cal, Fd	Clay	119		186	–	–

Qz: quartz; Fd: feldspar; Cal: calcite; Cli–Heu: clinoptilolite–heulandite; St: stilbite. (1) X-ray counts of the zeolite sample as received. (2) X-ray counts of the zeolite sample after heating at 450 °C overnight.

[a] Conditioned CLI-1, size range 0.10–0.25 mm.

[b] Conditioned CLI-1, size range 0.25–1.00 mm.

[c] CLI-1 after being used in the breakthrough studies with 0.01 M H_2SO_4.

inorganic cation exchangers that exhibit high ion exchange capacity, selectivity and compatibility with the natural environment [15].

Municipal wastewater is the main source of phosphate ions in the environment, whereas ammonium ion is ubiquous in municipal and agricultural wastewaters. Both ions are the responsible for eutrophication phenomena. Based on the high selectivity of clinoptilolite for ammonium, selective ion exchange has been considered as an alternative technology for ammonium removal from wastewater [16]. Moreover, the presence of high ammonium contents in the drinking water is also a main problem in many rural communities of some parts of South America where, on the other hand, natural zeolite deposits are especially abundant.

The aim of this paper is to assess the use of natural zeolites newly discovered in Ecuador and Brazil [17] for the clean up of AMD and municipal wastewaters. With this end, we have obtained the breakthrough curves for the cations Pb^{2+}, Cu^{2+}, Zn^{2+}, NH_4^+ and H^+ on different zeolite samples from these localities, in order to ascertain their effective ion exchange capabilities.

2. Experimental

2.1. Materials

The clinoptilolite–heulandite materials were obtained from zeolite-rich tuff samples mined in Guayaquil (Ecuador). These samples, all of them from the Andes mountains come from the same geological layer (Cayo Formation) but are mined from different sites. The stilbite materials were obtained from zeolite-rich tuff samples mined in the Parnaiba Basin (Brazil).

2.2. Characterization of the zeolites

The mineralogical composition of the zeolitic tuffs was determined by powder X-ray diffraction (XRD) analysis in a diffractometer Philips PW-1820 with Cu anode ($K_{\alpha 1}$ = 1.54 Å) scanning from $2\theta = 4^\circ$ to 60°. XRD allows also distinguishing between clinoptilolite and heulandite in the zeolitic tuffs by heating the samples at 450 °C overnight and registering the XRD pattern afterwards. Table 1 summarizes the mineralogical composition of the zeolitic tuffs, as well as the X-ray counts of their main diffraction peaks.

The bulk chemical composition of these zeolites (wt.%) was analyzed in a wavelength dispersive X-ray fluorescence spectrometer (XRF) Philips PW-1404 with Sc-Mo anode using powder pellets of the material, and is summarized in Table 2.

The BET surface, pore volume and pore size of the zeolitic tuffs was analyzed by isothermal N_2 adsorption in a Micromeritics ASAP-2010 instrument and the results are summarized in Table 3.

Table 2
Bulk chemical composition of the zeolitic tuffs (wt.%) by X-ray fluorescence analysis.

Sample	SiO_2	Al_2O_3	Fe_2O_3	CaO	Na_2O	MgO	K_2O	Si/Al	LOI[a]
HEU-1	66.54	12.77	4.27	2.45	1.71	1.40	0.39	4.60	9.10
HEU-2	58.15	14.12	6.57	3.68	1.54	1.99	1.28	3.63	11.80
CLI-1	66.00	11.49	2.69	3.42	1.98	0.77	0.34	5.05	12.80
STI-2	56.92	16.68	4.58	4.83	0.31	2.88	0.90	3.01	11.97
STI-1	68.79	11.71	5.25	3.34	2.75	1.31	0.62	5.15	5.84
CLI-2[b]	62.28	12.08	4.09	2.36	5.39	1.49	0.66	4.52	10.92
CLI-2[c]	65.80	11.32	3.42	1.23	4.10	0.96	0.45	5.11	12.29

[a] LOI: loss on ignition.

[b] Conditioned CLI-1, size range 0.10–0.25 mm.

[c] Conditioned CLI-1, size range 0.25–1.00 mm.

2.3. Cation exchange capacity (CEC)

The experimental CEC was determined from ion exchange experiments. For this purpose, the samples of dry zeolite (0.5 g of grain size below 45 μm) were placed in a centrifuge tube and mixed for 15 min with 30 mL of 1 M ammonium acetate solution. By this process NH_4^+ ions displaced most of the cations, converting the zeolite into the NH_4^+ form. The solution was centrifuged for 5 min at 2500 rpm, and the mother liquor was decanted in a 100-mL volumetric flask. This process was repeated twice in order to displace all the exchangeable ions from the zeolite lattice, since this is an equilibrium process, but mixing the NH_4^+ solution only for 5 min. The mother liquors were diluted to 100 mL with the ammonium acetate solution, and were analyzed for Na^+, K^+, Ca^{2+} and Mg^{2+} (exchangeable bases) by atomic absorption spectrometry (AAS) in a Philips PU 9100X spectrophotometer. After this exchange process, the zeolite samples were washed three times with 30 mL of 30 wt.% ethyl alcohol (mixing for 30 s and centrifuging for 2.5 min at 2500 rpm), dried to constant weight and mixed for 15 min with 30 mL of 10 wt.% potassium chloride solution to convert the zeolites back to the potassium form (regeneration process). The mixture was centrifuged for 5 min at 2500 rpm and the mother liquors

Table 3
BET Surface, pore volume and pore size of the zeolitic tuffs.

Sample	BET surface ($m^2\ g^{-1}$)	Pore volume ($cm^3\ g^{-1}$)	Pore size (Å)
HEU-1	13.52	0.0021	80.12
HEU-2	14.30	0.0067	112.40
CLI-1	76.84	0.0350	31.54
STI-2	19.04	0.0040	51.60
CLI-2[a]	123.23	0.0560	30.33

[a] Conditioned CLI-1, size range 0.10–0.25 mm.

Table 4
Cation exchange capacity (CEC) of the zeolitic tuffs (mequiv./100 g zeolite).

Sample	Na^+	K^+	Ca^{2+}	Mg^{2+}	CEC_{bases}[a]	CEC NH_4^+
HEU-1	0.91	0.80	3.45	12.40	17.56	32.10
HEU-2	3.50	0.90	10.50	16.10	31.00	49.80
CLI-1	63.56	0.83	22.10	10.53	97.02	151.50
STI-2	6.30	2.20	9.40	71.30	89.20	122.30
STI-1	2.80	2.20	5.50	80.80	91.30	76.60
CLI-2[b]	105.36	0.79	15.98	2.19	124.32	157.50

[a] $CEC_{bases} = \Sigma\,[Na^+] + [K^+] + [Ca^{2+}] + [Mg^{2+}]$.
[b] Conditioned CLI-1, size range 0.25–1.00 mm.

were decanted in a 100-mL volumetric flask. This process was repeated twice by the reason stated above, and the mother liquors were diluted to 100 mL with the potassium chloride solution. The amount of NH_4^+ ions that left the zeolite phase was determined by visible spectroscopy using the Nessler reagent [18] (λ = 420 nm) in a PerkinElmer Lambda-3 spectrophotometer. The CEC_{bases} and $CEC_{ammonium}$ are summarized in Table 4.

2.4. Breakthrough curves

Breakthrough studies were performed using 30 cm long × 2 cm outside diameter glass columns at ambient temperature. Each column was loosely packed with about 35 g of zeolitic tuff (of grain size in the range 0.25–1.00 mm) yielding bed depths of about 10 cm. Actual bed depths of each column were measured and used to calculate bed volumes (BV). Columns were operated under flooded conditions, charging the cation loading solution at the top of the column. The bottom outlet of the column was fitted with a control valve to regulate the flow rate of the effluent to around 1.4 BV h^{-1} (1 mL min^{-1}) (10 BV h^{-1} in the case of NH_4^+). Each column was loaded with a 0.01-M single cation solution using the following salts: lead nitrate, zinc sulphate monohydrate and copper sulphate pentahydrate, and a 0.0028 M solution of ammonium acetate (50 mg L^{-1} of NH_4^+). A 0.01 M solution of sulphuric acid was used in the H^+ breakthrough studies. The volume and pH of the column effluent were measured, and the effluent was analyzed for Na^+ and for the cation studied by AAS (for Pb^{2+}, Cu^{2+}, Zn^{2+}) and by visible spectroscopy for NH_4^+.

2.5. Conditioning of the zeolites with NaCl 2 M

Conditioning involved treating 10 g of the zeolites (of a grain size in the range 0.25–1.00 mm) with 100 mL of tap water to which 50 mg L^{-1} of Na^+ (as sodium chloride) and 100 mg L^{-1} of Ca^{2+} (as calcium chloride) were added [19]. The suspension was continuously mixed for a period of 24 h using a mechanical shaker equipped with variable speed engine. The suspension was left to settle and the liquid drained. The zeolites were mixed using 100 mL of a 2-M sodium chloride solution for 24 h after which most of the zeolites should be converted to the sodium form. Finally the solids were thoroughly washed with distilled water until all traces of Cl^- were removed, dried at 105 °C to constant weight and sieved to the desired size range. The mineralogical and bulk chemical compositions of the conditioned zeolites are given in Tables 1 and 2, and their BET surfaces areas and CEC's in Tables 3 and 4.

3. Theory and calculations

The ion exchange reaction is a stoichiometric process where one equivalent of an ion in the solid phase is replaced by one equivalent of an ion from solution. For binary ion exchange involving a monovalent cation (such as Na^+) and divalent cations M^{2+} (such as Pb^{2+}, Cu^{2+} and Zn^{2+}) the equilibrium reaction may be written as:

$$2Na_z^{+} + M_s^{2+} \leftrightarrow 2Na_s^{+} + M_z^{2+}$$

where the subscripts z and s refer to the zeolite and solution phases, respectively. For the determination of the experimental CEC of the zeolites, we have followed a well established and accepted method [19], that is, measuring the uptake of ammonium cation at room temperature when equilibrium conditions have been attained in the presence of 1 M ammonium salt solution. Of course, the theoretical CEC is much higher [20]. In the experiments with the zeolite columns, as the breakthrough test progressed, the test cation concentration in the effluent (C) abruptly increased and approached that of the loading solution (C_0) with a simultaneous drop in Na^+ concentration, demonstrating cessation of ion exchange. The point at which the test cation concentration in the effluent reached the 5% of the cation concentration in the loading solution ($C = 0.05 \cdot C_0$) was considered the "breakthrough point". This breakthrough point could be expressed in terms of breakthrough time, dividing the accumulated volume (mL) of 0.01 M cation test solution at breakthrough point by the flow rate (mL min^{-1}), or in terms of effective CEC (mequiv. g^{-1}), dividing the milliequivalents (mequiv.) of test cation determined from the accumulated volume of 0.01 M solution at the breakthrough point by the number of grams of zeolitic tuff in the column. The graphical plot of C/C_0 vs. time (or mequiv. g^{-1}) is called the breakthrough curve.

The results that can be obtained from each breakthrough curve are:

- The breakthrough time, t_b in hours.
- The weight of test cation exchanged per gram of zeolite until the breakthrough time, W_b (mg cation/g zeolite) [21].

$$W_b = \frac{F_A \int_0^{t_b} (1 - (C/C_0))\ dt}{d \cdot h} \quad (1)$$

where d = apparent density of the zeolite (g cm^{-3}), h = length of the zeolite bed (cm), F_A = test cation feed rate per square centimeter of column section (g cm^{-2} h^{-1}) [21].

$$F_A = \frac{Q \cdot C_0}{1000 \cdot S} \quad (2)$$

Q is the flow volume of the test cation solution (cm^3 h^{-1}), C_0 is the concentration of the test cation in the loading solution (g cm^{-3}), S is the breakthrough column section (cm^2), $\int_0^{t_b}(1 - C/C_0)\,dt$ = area limited by the breakthrough curve, the abscissa in time units (h) and the ordinate $C/C_0 = 1$. The upper limit of integration is the breakthrough time, t_b.

The Figs. 1–5 show the breakthrough curves of Pb^{2+}, Cu^{2+}, Zn^{2+}, H^+ and NH_4^+ for the four zeolitic tuffs tested, and the Na^+ concentration in the effluent of the CLI-1 column.

4. Results and discussion

4.1. Results of the characterization of the zeolitic tuffs

The family of zeolites containing the heulandite or HEU topology is the most abundant of the zeolites found in nature [1,2]. These natural minerals are found with Si/Al ratios ranging between 3 and 5. The higher silica member of this family is identified as clinoptilolite, with a Si/Al ratio greater than 4. Heulandites are defined as those minerals with Si/Al ratio below 4. In our samples, the presence in the zeolitic tuffs of variable amounts of quartz and feldspar somewhat makes difficult to apply these classification criteria. However, CLI-1 is the sample with the highest Si/Al ratio (5.05) with lower Si/Al ratios for HEU-2 (3.63) and HEU-1 (4.60). The key difference between natural heulandite and clinoptilolite is their

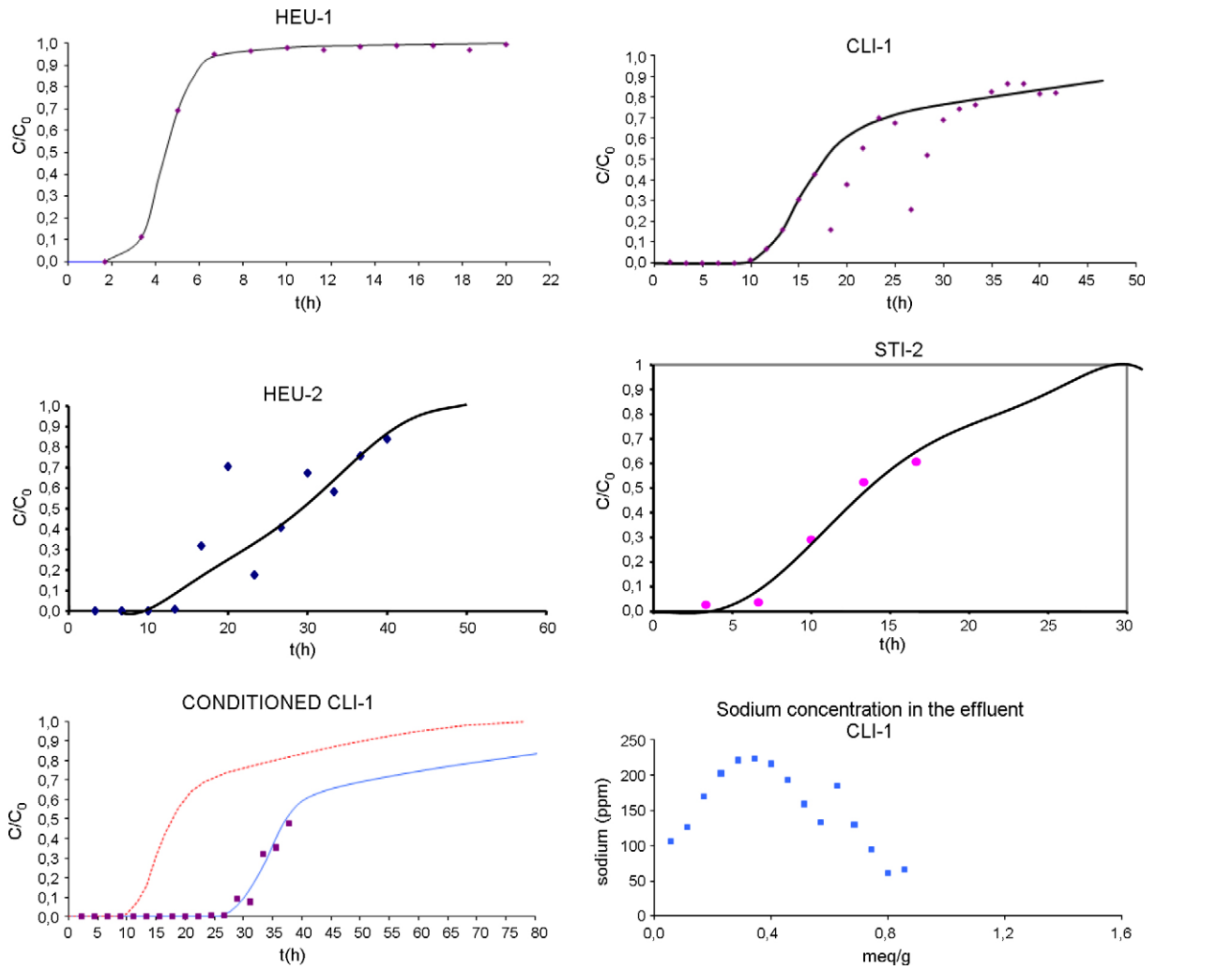

Fig. 1. Breakthrough curves for Pb^{2+} on the four natural zeolitic tuffs and on the CLI-1 conditioned with 2 M NaCl (in this latter case, the red line shows the curve on the natural zeolite for easier comparison). The bottom right curve shows the Na^+ concentration in the effluent of the natural CLI-1 zeolitic tuff. (For interpretation of the references to color in this figure legend, the reader is referred to the web version of the article.)

thermal stability. Clinoptilolite is thermally stable to temperatures in excess of 500 °C, while heulandite undergoes structural collapse by 350 °C [22]. Thus, we have heated the clinoptilolite–heulandite tuffs at 450 °C for 12 h; the CLI-1 sample keeps the crystallinity unchanged showing its clinoptilolite nature, whereas the HEU-1 and HEU-2 samples collapse totally under heating, resulting to be heulandites (see Table 1 and Fig. 6). The zeolitic tuff from Brazil has been unequivocally identified as stilbite by XRD. The theoretical Si/Al ratio for stilbite is 3.00; the sample STI-2 has exactly this Si/Al ratio (3.01) although its XRD pattern shows the presence of minor amounts of quartz and clay. The sample STI-1 has a higher Si/Al ratio of 5.15 due to the presence of a large amount of quartz, and on this ground it was discarded for the breakthrough experiments.

The BET surface of the sample CLI-1 is by far the largest of the four zeolitic tuffs, as well as its pore volume being at least an order of magnitude higher than those of the other zeolitic tuffs. The pore size of the CLI-1 sample is the smallest in the group (31.5 Ã), and it does not change with the conditioning process (30.3 Ã) showing the true zeolitic nature of the tuff. The CEC of the sample CLI-1 is also the higher in the group; it is especially noteworthy its high content of exchangeable Na^+ (63.56 mequiv./100 g zeolite) when compared with the rest of the zeolitic tuffs (Table 4). The difference between the CEC_{bases} (lower in all the cases except for STI-1) and the $CEC_{ammonium}$ could be due to the presence of exchangeable cations as Fe^{3+} different from the analyzed cations Na^+, K^+, Ca^{2+} and Mg^{2+}.

4.2. Discussion of results of the breakthrough studies

Table 5 summarizes the parameters t_b and W_b (see Section 3) for the test cations Pb^{2+}, Cu^{2+}, Zn^{2+}, H^+ and NH_4^+ on the four zeolitic

Table 5
Breakthrough values for the zeolitic tuffs.

Ionic species	HEU1	HEU-2	CLI-1	STI-2	CLI-2[a]
Breakthrough time, t_b (h)					
Pb^{2+}	2.42	12.00	11.11	5.70	28.67
Cu^{2+}	1.93	6.50	0.75	3.40	21.20
Zn^{2+}	1.16	2.00	0.70	3.40	6.00
H^+	15.17	50.00	19.56	6.70	13.99
NH_4^+	0.33	8.00	15.00	10.40	n.d.
Cation exchange capacitiy, W_b (mg g^{-1})					
Pb^{2+}	8.60	20.40	40.40	8.76	73.40
Cu^{2+}	2.10	3.94	0.80	2.05	19.20
Zn^{2+}	2.00	2.67	1.20	3.03	7.80
H^+	0.52	7.64	0.67	1.01	0.48
NH_4^+	0.14	0.34	6.40	0.44	n.d.

[a] Conditioned CLI-1, size range 0.10–0.25 mm.

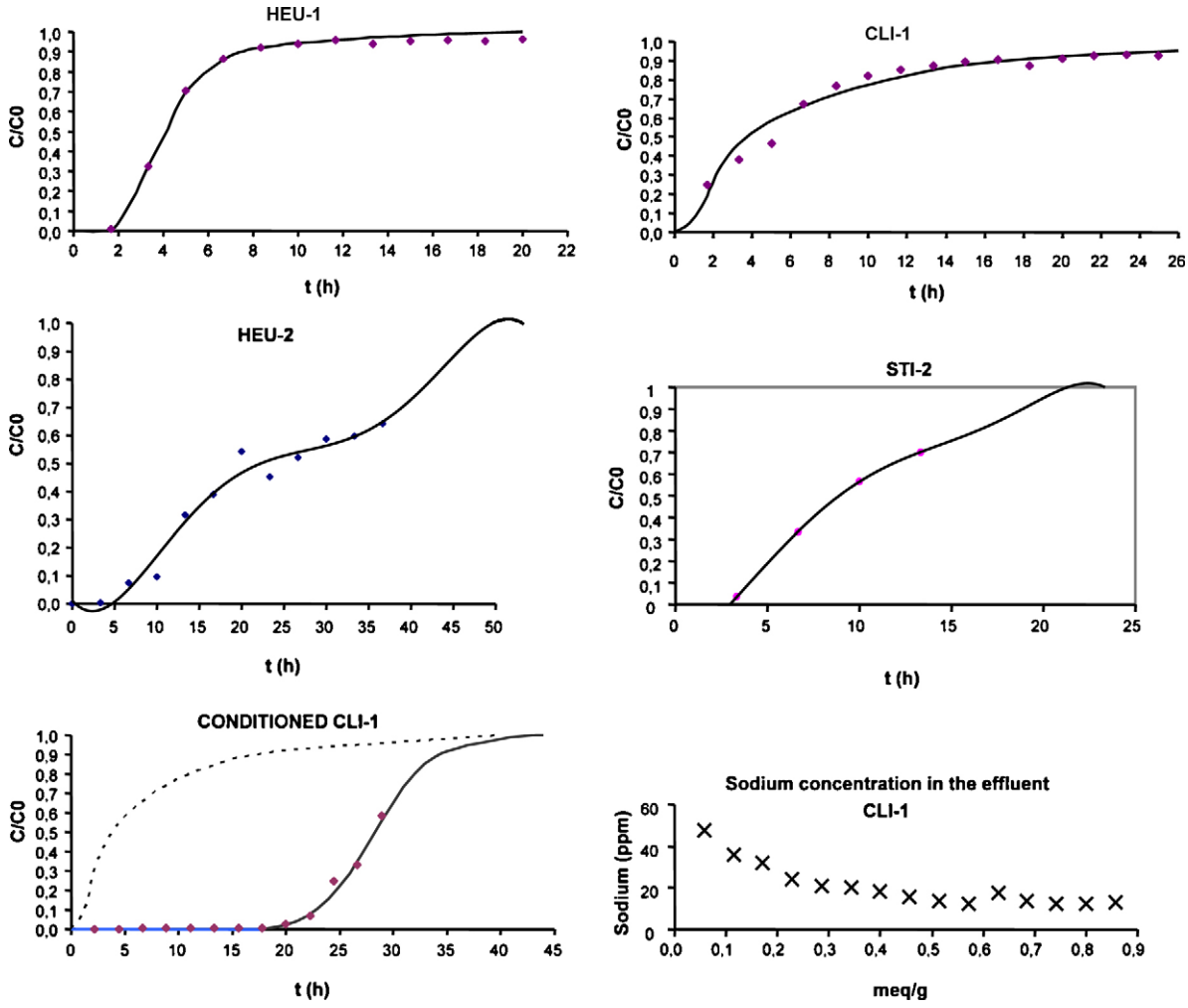

Fig. 2. Breakthrough curves for Cu^{2+} on the four natural zeolitic tuffs and on the CLI-1 conditioned with 2 M NaCl (in this latter case, the dashed line shows the curve on the natural zeolite for easier comparison). The bottom right curve shows the Na^+ concentration in the effluent of the natural CLI-1 zeolitic tuff.

tuffs tested as received and for the zeolite CLI-1 conditioned with NaCl 2 M. The data from the breakthrough curves were used to determine the order of cation affinity of the four zeolitic tuffs for cations typically found in the AMD from the Iberian pyritic belt. The curves were developed for each of the test cations with each of the zeolite samples. The Figs. 1–5 show the breakthrough curves of Pb^{2+}, Cu^{2+}, Zn^{2+}, H^+ and NH_4^+ for the four zeolitic tuffs tested, and the Na^+ concentration in the effluent of the CLI-1 column. The shape of the Na^+ curve is a mirror image of the breakthrough curve for each added cation, and indicates the equivalent exchange of Na^+ for the cation. pH is presented instead of H^+ concentration in the Fig. 4 for the H^+ breakthrough curve. The apparent breaks in the curves we attributed to the interruption in the experiments over the weekends, allowing for equilibration between solution cation and ion-exchanged cation to occur.

In single cation solution containing no competing cations, the breakthrough time t_b is a relative measure of the affinity for that particular cation; the greater the loading prior to breakthrough, the greater the apparent affinity. Table 5 summarizes the data for the breakthrough studies that allows to predict the following orders of affinity for single cation solutions based in the breakthrough time:

Zeolite HEU-1: $H^+ > Pb^{2+} > Cu^{2+} > Zn^{2+}$
Zeolite HEU-2: $H^+ > Pb^{2+} > Cu^{2+} > Zn^{2+}$
Zeolite CLI-1: $H^+ > Pb^{2+} > Cu^{2+} = Zn^{2+}$
Zeolita STI-2: $H^+ > Pb^{2+} > Cu^{2+} = Zn^{2+}$

For all the four zeolite samples, the orders of affinity indicate that H^+ and Pb^{2+}, in this order, are preferred over Cu^{2+} and Zn^{2+}; for the zeolites HEU-1 and HEU-2 the affinity for Cu^{2+} is slightly higher than for Zn^{2+}, but the samples CLI-1 and STI-2 show identical affinity for these latter cations.

These selectivity series could be the result of various factors which influence the ion exchange behaviour in zeolites. One factor is the framework structure of the zeolite itself. The dimensions of the channel formed by the tetrahedrical units which make up the zeolite must be large enough to allow the passage of a metal ion. A common factor that prevents the ion being exchanged by a zeolite is the size of the ion. If the size of the ion is greater than that of the pore the species will be excluded [19]. By comparison of the hydrated ion sizes of the metals examined [23,24] (Table 6), the following selectivity sequence is generated:

$$H^+ > Pb^{2+} > Cu^{2+} > Zn^{2+}$$

Table 6
Radii and hydration energies for metal cations [27].

Cation	Hydrated radius (Å)	Unhydrated radius (Å)	Free energy of hydration (kJ/mol-ion)
Cu^{2+}	4.19	0.73	−2 021.9
Zn^{2+}	4.30	0.74	−1 969.2
Pb^{2+}	4.01	1.32	−1 435.6
H^+	2.80	1.15	−1 063.0

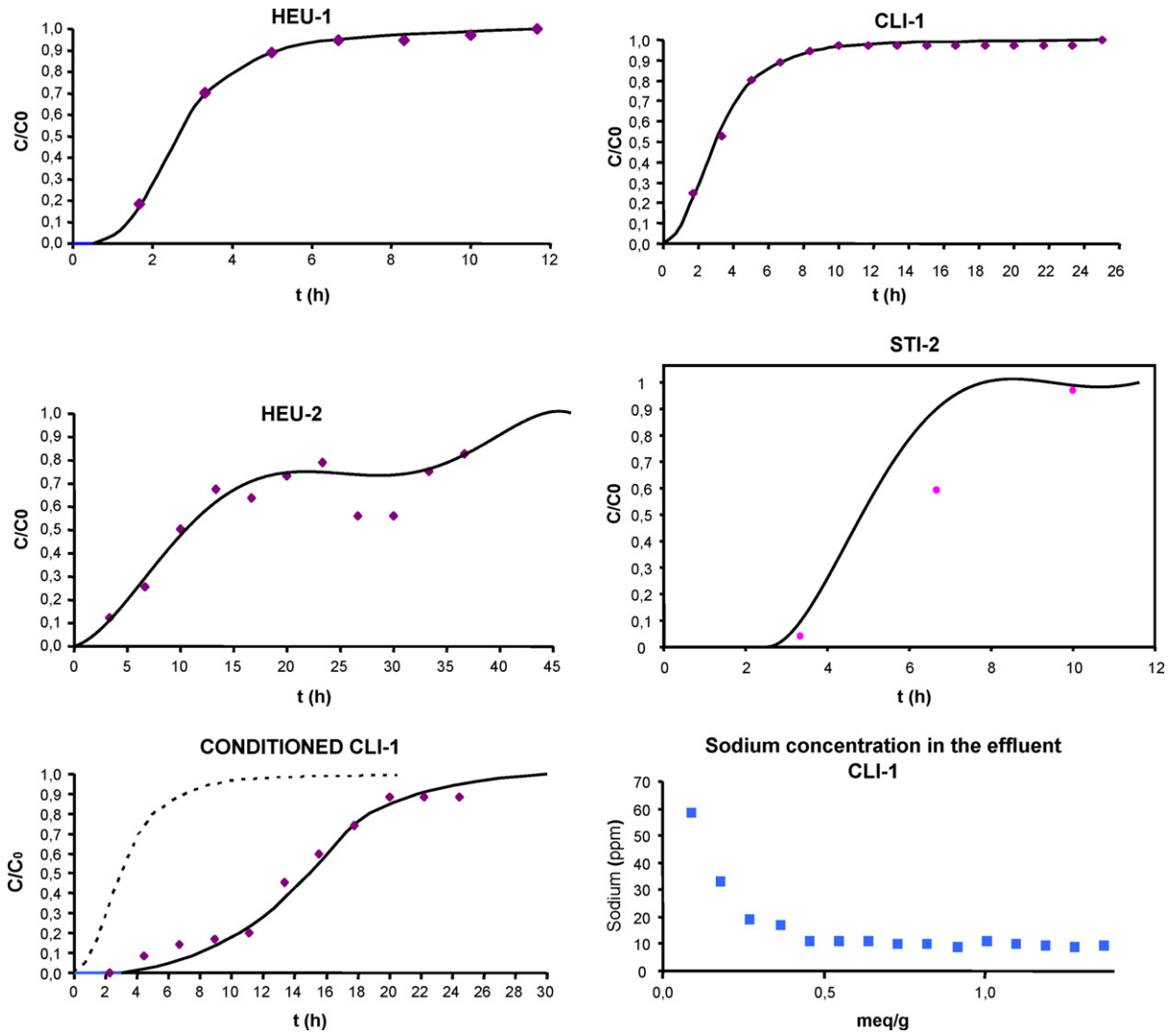

Fig. 3. Breakthrough curves for Zn^{2+} on the four natural zeolitic tuffs and on the CLI-1 conditioned with 2 M NaCl (in this latter case, the dashed line shows the curve on the natural zeolite for easier comparison). The bottom right curve shows the Na^{+} concentration in the effluent of the natural CLI-1 zeolitic tuff.

Very similar to the one produced by the experimental tests in all the zeolitic tuffs.

The other factor influencing ion exchange behaviour in zeolites is the cation free energy of hydration and their electrostatic bond energies. Eisenman [25] has shown that the specificity of a surface containing fixed charges for alkali metal ions can be accounted for in terms of ion hydration and electrostatic bond energies. Sherry [26] extended this model for divalent ions. According to this model, if a cation exchanger such as a zeolite is placed in a solution containing different metal salts, the preference of the zeolite for one metal over another depends on whether the difference in their hydration free energy or Coulombic free energy of interaction with fixed anionic exchange sites predominates. Since the Si/Al ratio in clinoptilolite is relatively high, 4.25–5.25, and the volumetric capacity is low, the ionic field within the zeolite structure is relatively weak, and the electrostatic interactions are not expected to be as important as hydration free energy. The cations with the highest (absolute value) free energy of hydration should therefore prefer to remain in the solution phase where their hydration requirements may be better satisfied. According to the hydration energies listed in the Table 6 [27], the selectivity series for the cations considered should be also:

$$H^{+} > Pb^{2+} > Zn^{2+} > Cu^{2+}$$

This hydration energy model does explain the much higher selectivity of clinoptilolite for H^{+} and Pb^{2+}, and the similar values found in the experimental tests for Cu^{2+} and Zn^{2+}.

The maximum adsorption capacity of the zeolites for cation removal until breakthrough time (W_b, mg g^{-1}) is also shown in Table 5. For the removal of Cu^{2+} and Zn^{2+} these values are similar to those reported in the literature for clinoptilolite (3.8 and 2.7 mg g^{-1} for Cu^{2+} and Zn^{2+}, respectively); only CLI-1 show both values surprisingly low. For the removal of Pb^{2+}, the zeolites HEU-1 and STI-2 show values similar to the reported ones (6.0 mg g^{-1}), but HEU-2 and CLI-1 show values exceedingly higher, 20.4 and 40.4 mg g^{-1}, respectively, three and seven times, respectively the literature values [19,28,29]. Thus, both zeolites and especially CLI-1 would be very selective for the removal of Pb^{2+}.

After pretreating the as-received CLI-1 sample with a 2 M NaCl solution (conditioning), the breakthrough time increased from 0.70 to 21.20 h and 6.00 h for Cu^{2+} and Zn^{2+}, respectively, with a lower relative increase for Pb^{2+} from 11.11 to 28.67 h, and a decrease for H^{+}, demonstrating that measured exchange capacities of as-received zeolitic tuffs may not accurately reflect their potential exchange capacities for AMD. This is particularly true for the removal of Cu^{2+} and Zn^{2+}, where the conditioned CLI-1 sample shows adsorption capacities (19.9 and 7.80 mg g^{-1}) much higher than those reported in the literature for clinoptilolite [19,28,29].

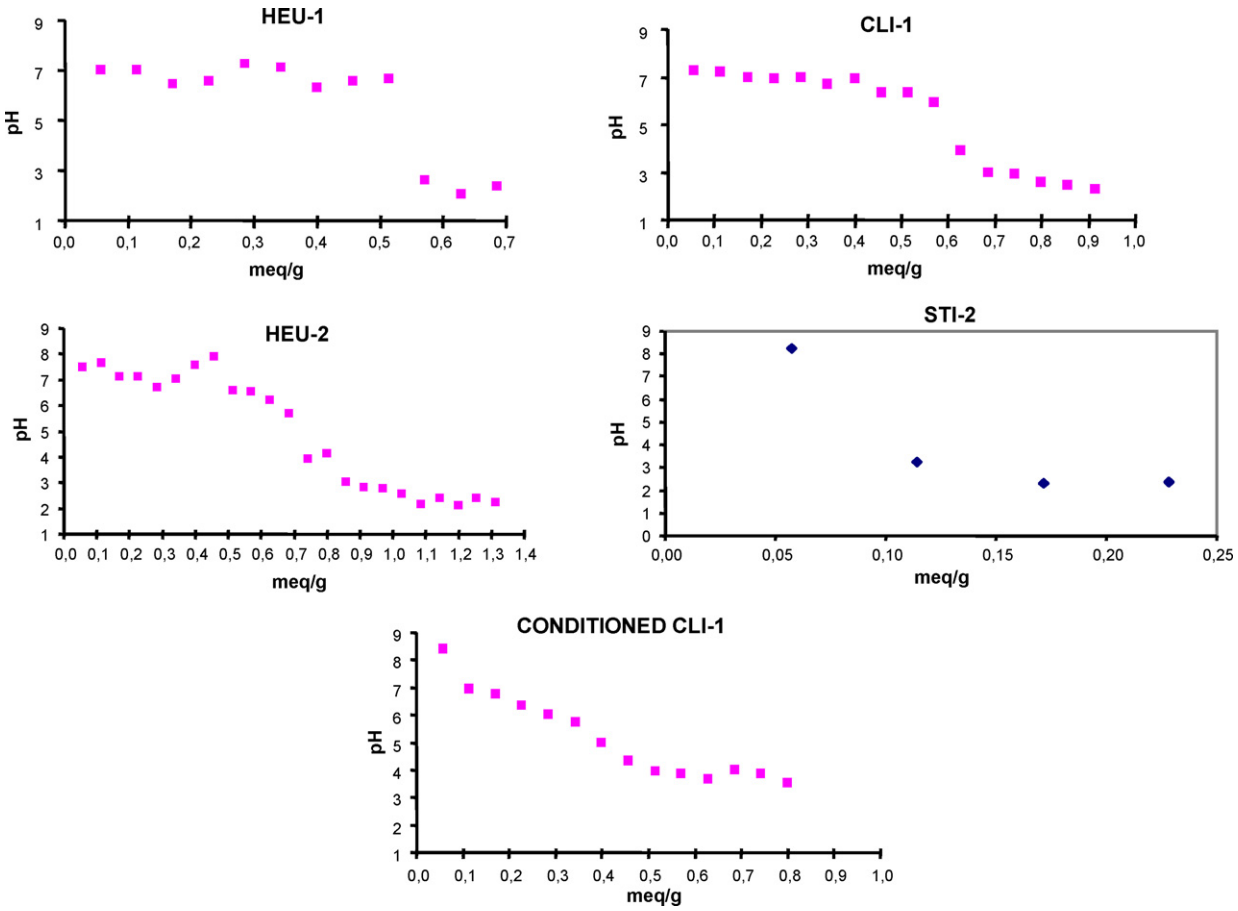

Fig. 4. Breakthrough curves for H^+ on the four natural zeolitic tuffs and on the CLI-1 conditioned with 2 M NaCl (pH is plotted instead of H^+ concentration).

Metal removal efficiency using zeolites could be affected by the solution pH. However, the solution pH affected to a minimum extent the removal of Cu^{2+}, Zn^{2+} and Pb^{2+} [19]. The elution of a solution of 0.01 M H_2SO_4 through the zeolites does not affect its crystalline structure (see Table 1, last entry), showing a difference with other zeolites whose crystalline structures collapse after passing acidic solutions through them.

CLI-1 zeolite showed also a good efficiency for NH_4^+ removal, 6.40 mg g^{-1} at the higher elution rate of 10 BV h^{-1}, followed at a great distance by STI-2, HEU-2 and HEU-1 (see Table 5). The Fig. 5

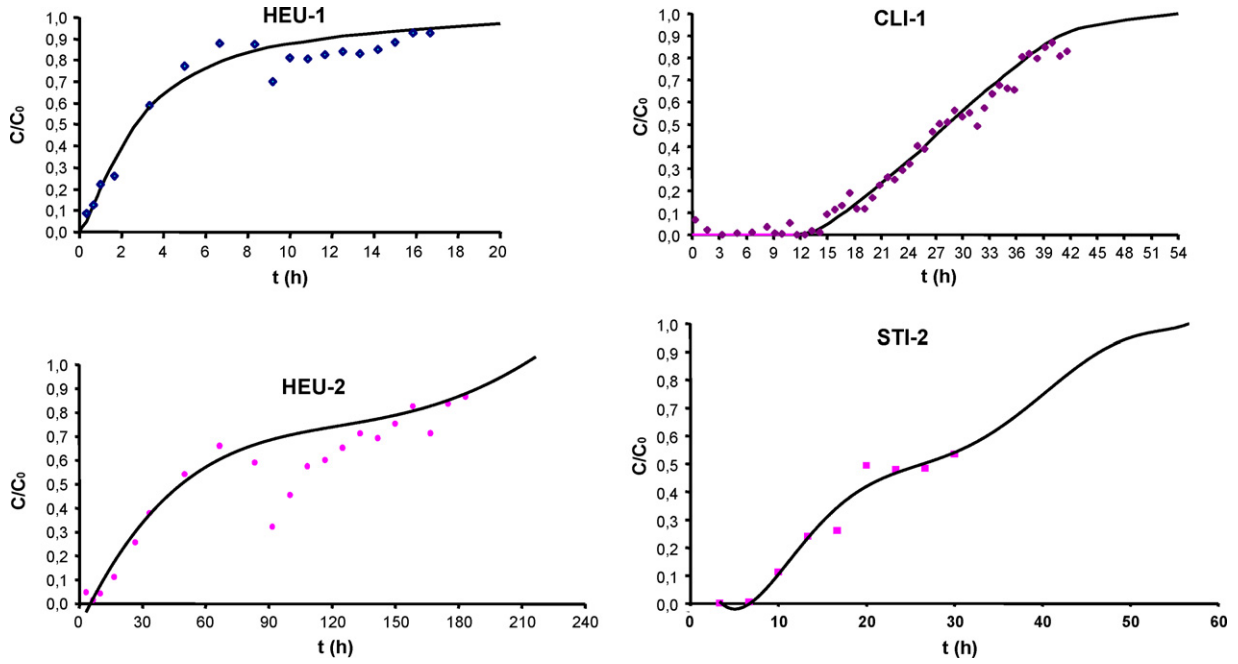

Fig. 5. Breakthrough curves for NH_4^+ on the four natural zeolitic tuffs.

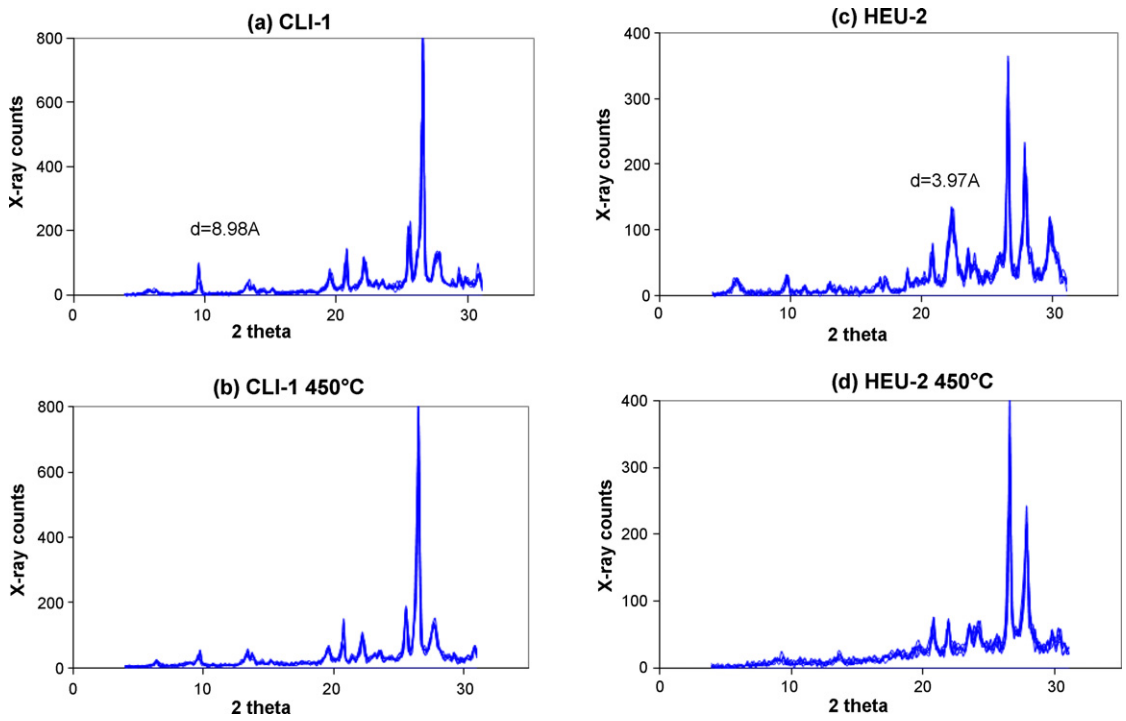

Fig. 6. (a) XRD pattern of CLI-1 zeolitic tuff as received; (b) XRD pattern of CLI-1 zeolitic tuff heated at 450 °C for 12 h; (c) XRD pattern of HEU-2 zeolitic tuff as received; (d) XRD pattern of HEU-2 zeolitic tuff heated at 450 °C for 12 h. In all cases, only the scanning from $2\theta = 4°$ to $2\theta = 30°$ is shown.

shows the breakthrough curve for NH_4^+ over the four zeolitic tuffs. An ion exchange study of clinoptilolite [30] showed that NH_4^+ ion is preferred over Na^+, and that Na^+ was preferred over the divalent cations Zn^{2+}, Cu^{2+} and Cd^{2+}. This study also showed that although there was some ion sieving with Pb^{2+}, it was preferred to Na^+. As it can be deduced from the above discussion, our results agree very well with this study.

5. Conclusions

The order of effective cation-exchange capacity for the zeolitic tuffs studied, as determined from the breakthrough curves and from Table 5, is:

$$CLI - 1 > HEU - 2 > HEU - 1 > STI - 2$$

This could be considered a general order because it is true for most of the cations studied. Thus, the ionic exchange on these natural zeolites could be an economically affordable, environmentally compatible and highly selective and effective way of removing cations, usually found in acid mine drainage and municipal and agricultural wastewaters, in some parts of the world where zeolite deposits are especially abundant.

Acknowledgement

We wish to thank to the Department of Chemical Engineering of the Universidad Complutense of Madrid for the analysis of BET surface, pore volume and pore size.

References

[1] G. Gottardi, E. Galli, Natural Zeolites, Springer-Verlag, Berlin, 1985.
[2] D. Zhao, K. Cleare, C. Oliver, C. Ingram, D. Cook, R. Szostak, L. Kevan, Characteristics of the synthetic heulandite–clinoptilolite family of zeolites, Micropor. Mesopor. Mater. 21 (1998) 371–379.
[3] N.V. Elizondo, E. Ballesteros, B.I. Kharisov, Cleaning of liquid radioactive wastes using natural zeolites, Appl. Radiat. Isotopes 52 (2000) 27–30.
[4] C. Constantopoulou, M. Loizidou, Z. Loizou, N. Spyrellis, Thorium equlibria with the sodium form of clinoptilolite and mordenite, J. Radioanal. Nucl. Chem. 178 (1994) 143–151.
[5] S. Kesraoni-Ouki, C.R. Cheeseman, R. Perry, Natural zeolites utilisation in pollution control: a review of applications to metals' effluents, J. Chem. Tech. Biotechnol. 59 (1994) 121–126.
[6] A. Shanableh, A. Kharabsheh, Stabilization of Cd, Ni and Pb in soil using natural zeolite, J. Hazard. Mater. 45 (1996) 207–217.
[7] E. Malliou, M. Liozidou, N. Spyrellis, Uptake of lead and cadmium by clinoptilolite, Sci. Total Environ. 149 (1994) 139–144.
[8] A. Papadopoulos, E.G. Kapetanios, M. Liozodou, Studies on the use of clinoptilolite for ammonia removal from leachates, J. Environ. Sci. Health A: Environ. Sci. Eng. Toxic Hazard. Subst. Control 31 (1) (1996) 211–220.
[9] F. Nai-quian, Y. Hsi-ming, L. Zu, The strength effect of mineral admixture on cement concrete, Cem. Concr. Res. 18 (1998) 464–472.
[10] D. Fragoulis, E. Chaniotakis, M.G. Stamatakis, Zeolitic tuffs of Kimonos Island, Aegean Sea, Greece and their industrial potential, Cem. Concr. Res. 27 (1997) 889–905.
[11] V. Naidenov, Rapid hardening cement–gypsum composites for shot-crating on the base of Bulgarian raw materials, Cem. Concr. Res. 21 (1991) 896–904.
[12] F.A. Mumpton, Natural zeolites: a new industrial mineral commodity, in: L.B. Sand, F.A. Mumpton (Eds.), Natural Zeolites: Occurrence, Properties, Use, Pergamon Press, Oxford, 1976.
[13] P.R. Bremmer, L.E. Schultze, Ability of clinoptilolite-rich tuffs to remove metal cations commonly found in acidic drainage, in: D.W. Ming, F.A. Mumpton (Eds.), Natural Zeolites'93, Int. Comm. Natural Zeolites, Brockport, New York, 1993, pp. 397–403.
[14] W.W. Eckenfelder, Industrial Water Pollution Control, second ed., McGraw Hill, New York, 1989.
[15] S.K. Ouki, M. Kavannagh, Treatment of metals-contaminated wastewaters by use of natural zeolites, Water Sci. Technol. 39 (1999) 115–122.
[16] L. Liberti, A. López, V. Amicarelli, G. Boghetich, Phosphorous removal from wastewater using clinoptilolite: a review of the "Rim-nut" process, in: D.W. Ming, F.A. Mumpton (Eds.), Natural Zeolites'93, Int. Comm. Natural Zeolites, Brockport, New York, 1993, pp. 351–362.
[17] L. Machiels, F. Morante, R. Snellings, B. Calvo, L. Canoira, C. Paredes, J. Elsen, Zeolite mineralogy of the Cayo formation in Guayaquil, Ecuador, Appl. Clay Sci. (2008), doi:10.1016/j.clay.2008.01.012.
[18] L.S. Clesceri, A.E. Greenberg, R.R. Trussell (Eds.), Standard Methods for the Examination of Water and Wastewater (seventeenth ed.), American Public Health Association (APHA), Water Environment Federation (WEF), American Water Works Association (AWWA), Washington, DC, 1989, p. 4–117.
[19] S.K. Ouki, C.R. Cheeseman, M. Kavannagh, C.J. Sollars, R. Perry, The Application of Natural Zeolites in Pollution Control, Centre for Environmental Control and Waste Management, Imperial College of Science, Technology and Medicine, London, 1994.

[20] A. Dimirkou, M.K. Doula, Use of clinoptilolite and an Fe-overexchanged clinoptilolite in Zn^{2+} and Mn^{2+} removal from drinking water, Desalination 224 (2008) 280–292.
[21] W.L. McCabe, J.C. Smith, P. Harriot, Unit Operations of Chemical Engineering, Sixth ed., McGraw-Hill, New York, 2001.
[22] G. Gianetto-Pace, A. Montes-Rendón, G. Rodríguez-Fuentes, Zeolitas, Caracterización, Propiedades y Aplicaciones Industriales, Editorial Innovación Tecnológica, Caracas (2000), 351 pp.

It is a single volume book with 351 pp.

[23] A.G. Volkov, S. Paula, D.W. Deamer, Two mechanisms of permeation of small neutral molecules and hydrated ions across phospholipids bilayers, Bioelectrochem. Bioenerg. 42 (1997) 153–160.
[24] R.D. Shannon, Revised effective ionic radii and systematic studies of interatomic distances in halides and chalcogenides, Acta Crystallogr. A 32 (1974) 751–767.
[25] G. Eisenman, Cation selective glass electrodes and their mode of operation, Biophys. J. Supp. 2 (1962) 258–323.
[26] H.S. Sherry, The ion-exchange properties of zeolites, Chap. 3, in: J.A. Marinsky (Ed.), Ion exchange 2, vol. 2, Marcel Dekker, New York, 1969.
[27] D. Asthagiri, L.R. Pratt, M.E. Paulaitis, S.B. Rempe, Hydration Structure and free energy of biomolecularly specific aqueous dications, including Zn^{2+} and First Transition row metals, J. Am. Chem. Soc. 126 (4) (2004) 1285–1289.
[28] D. Langella, M. Pausini, P. Cappelletti, B. de Gennaro, M. de Gennaro, C. Colella, NH_4^+, Cu^{2+}, Zn^{2+}, Cd^{2+}, Pb^{2+} exchange for Na^+ in a sedimentary clinoptilolite, North Sardinia, Italy, Micropor. Mesopor. Mater. 37 (2000) 337–343.
[29] R. Petrus, J. Warchol, Ion exchange equilibria between clinoptilolite and aqueous solutions of Na^+/Cu^{2+}, Na^+/Cd^{2+} and Na^+/Pb^{2+}, Micropor. Mesopor. Mater. 61 (2003) 137–146.
[30] H.S. Sherry, Ion exchange, in: S.M. Auerbach, K.A. Carrado, P.K. Dutta (Eds.), Handbook of Zeolite Science and Technology, Marcel Dekker, New York, 2003, pp. 1007–1061.